Journal of Solid Mechanics Vol. 2, No. 3 (2010) pp. 231-247

Finite Element Modeling of Crack Initiation Angle Under Mixed Mode (I/II) Fracture

S.S. Bhadauria[1,*], K.K. Pathak[2], M.S. Hora[1]

[1]*Department of Applied Mechanics, Maulana Azad National Institute of Technology Bhopal, India*
[2]*Advanced Materials Processes Research Institute (CSIR), Bhopal India*

Received 8 June 2010; accepted 16 September 2010

ABSTRACT

Present study deals with the prediction of crack initiation angle for mixed mode (I/II) fracture using finite element techniques and *J*-Integral based approach. The FE code ANSYS is used to estimate the stress intensity factor numerically. The estimated values of SIF were incorporated into six different crack initiation angle criteria to predict the crack initiation angle. Single edge crack specimens of Araldite-Hardener were used for the present analysis. Load was applied up to critical limit of the specimens containing crack at different angles of inclination. The crack initiation angle obtained using stress intensity factor and *J*-integral based approach were found close to each other and also found to be in good agreement with the available experimental results in literature. It is also investigated that as crack inclination angle increases material was found to behave in a brittle manner.

Keywords: Finite element method; Mixed mode fracture; Stress intensity factor; *J*-Integral; Crack initiation angle; Fracture criteria

1 INTRODUCTION

THE research on the mixed fracture criterion and crack growth is significant in fracture mechanics and engineering. Many research works in this area have been conducted and some criteria for predicating the direction of the crack initiation angle and the critical fracture load of materials have been determined. Thus, studying crack initiation angles is an important issue in dealing with crack arrest. Accordingly, several criteria have been proposed to predict the crack initiation angle. These criteria can be categorized on the basis of the critical parameter on which the criterion is defined. These parameters might be a critical value of stress, energy or strain. Griffith [7] was the first to propose a crack initiation criterion based on energy. On the other hand, Erdogan and Sih [6] were the first to propose a crack initiation criterion, the so called the maximum tangential stress (MTS) criterion, using the stress as a critical parameter. To support their criterion, Erdogan and Sih [6] conducted experiments using brittle Plexiglas plates and it is believed that MTS is suitable for analyzing brittle material. Later, Sih [17, 18] used the strain as a critical parameter in order to propose the minimum strain energy density (S) criterion. The (S) criterion showed a good agreement with the experimental results obtained earlier by Erdogan and Sih [6]. In addition, this criterion is the only one that shows the dependence of the initiation angle on material property represented by Poisson's ratio ν. Similar to Sih, Theocaris et al. [21-23] used the strain as a critical parameter to propose the maximum dilatational strain energy (T) criterion. Theocaris et al. [21-23] used Polycarbonate specimens for their experimental work and their experimental results showed a good agreement with the theoretical predictions. On the other hand, Kong et al. [11] proposed the maximum triaxial stress (M) criterion which uses the stress as a critical parameter. Kong et al. [11] experimental results were in agreement with the theoretical predictions as well as the experimental results by Theocaris et al. [21-23]. Ukadgaonker and Awasare [25] presented the T-criterion in a new

* Corresponding Author. Tel.:+91 8120 056572.
E-mail address: ssb.aero@gmail.com (S.S. Bhadauria).

form using the first and second stress invariants. Shafique and Marwan [19] modified the MTS criterion in order to be suitable for analyzing ductile materials. To achieve this, they introduced a variable radius for the plastic core region and used the von Mises yield criterion for determining the variable radius. Later, Shafique and Marwan [20] proposed the (R) criterion.

Computation of fracture parameters, such as the stress intensity factors or energy release rate, using finite element analyses requires either a refined mesh around the crack tip or the use of "special elements" with embedded stress singularity near the crack tip. Although conceptually the stress intensity factors are obtained in a straightforward approach, finite elements analyses with conventional element near the crack tip always underestimate the sharply rising stress-displacement gradients. Instead of trying to capture the well-known $1/\sqrt{r}$ singular behavior with very small elements, Hanshell and Shaw [8] and Barsoum [3, 4] proposed a direct method by shifting the mid-side node of an 8-noded isoparametric quadrilateral element to the one-quarter point from the crack tip node. Relocating the mid-side nodes to the one-quarter point achieves the desire $1/\sqrt{r}$ singular behavior. As an extension of the node collapsing approach Pu et al. [13] showed that the stress intensity factors K_I and K_{II} for opening and sliding modes, respectively, can be calculated directly from the nodal displacement on the opposite sides of the crack plane. Peter et al. [14] developed a finite element program which combines the analytical crack tip solution with a conventional finite element analyses. Petit et al. [15] used finite element method to obtain the displacement field in order to evaluate the stress intensity factors (K_I and K_{II}) and simulate the crack propagation for an inclined edge crack panel with crack angle of 45º. Rousseau and Tippur [16] studied the mixed mode crack tip deformation and developed a FE model using ANSYS and validated their model by their measurements. Ayhan [2] used three-dimensional enriched finite elements to calculate mixed mode stress intensity factors for deflected and inclined surface cracks in finite-thickness plates under uniform tensile remote loading. Tilbrook et al. [24] modified the finite element model which was used for simulating mixed-mode crack propagation in a linear elastic material to incorporate yielding. Joch and Ptak [9] examined several methods for 2D quasi-static linear-elastic problems to compute the stress intensity factor under mixed-mode mechanical loading conditions. Cherapanov [5] defined the components of two dimensional *J*-Integral problems.

In this paper, mixed mode finite element analyses were carried out on five specimens using Araldite-Hardener. The final crack length was kept 27.5 mm for all the specimens and crack inclination angle was taken to 0˚, 15˚, 30˚, 45˚ and 50˚. The crack tip radius *r* (distance from crack tip) was taken 0.8 mm. To vary the *a/w* ratio, crack length was varied by keeping the width of the specimen constant. The mixed mode stress intensity factors K_I and K_{II} was determined. Using the values of SIF obtained, crack initiation angle was calculated using six different criterions.

2 TEST MATERIAL AND SPECIMEN

Material used for the analysis was Araldite-Hardener. Single edge crack specimen dimensions of 117×41×6.5 mm were considered for the study. The crack was inclined at different inclination angle namely 0˚, 15˚, 30˚, 45˚ and 50˚; the final crack length was taken to 25.5 mm but it is varied by changing the *a/w* ratio from 0.1 to 0.7 to study the geometry effect. The crack tip radius *r* (distance from crack tip) was taken to 0.8 mm. To find out the proportionality limits, and Young's modulus, a rectangular shaped specimen of 117×41×6.5 mm size, was loaded on computerized Zwick/Roell Universal Testing Machine, model Z250 of 25 kN capacity with a crosshead speed 1 mm/min. The program for tensile test was loaded in the console control to obtain the proportionality limits and modulus of elasticity to 1.99×10^5 GPa. To obtain the Poisson's ratio an extensometer Biaxial Model of Gage length 25 mm, travel ±2.5mm axial/ ±1 mm transverse from Epsilon Technology Corp was used to obtain the lateral and longitudinal extensions. These values were then used to obtain the Poisson's ratio which came out to be 0.36.

3 CRACK INITIATION ANGLE CRITERION

3.1 MTS criterion

Erdogan and Sih [6] were the first to propose a crack initiation criterion using the stress as a critical parameter. This criterion states that direction of crack initiation coincides with the direction of the maximum tangential stress along a constant radius around the crack tip so it is called the maximum tangential stress (MTS) criterion. It can be stated mathematically as:

$$\begin{cases} \dfrac{\partial^2 \sigma_\theta}{\partial^2 \theta} < 0 \\ \dfrac{\partial \sigma_\theta}{\partial \theta} = 0 \end{cases} \tag{1}$$

$$\tan^2\frac{\theta}{2} - \frac{\mu}{2}\tan\frac{\theta}{2} - \frac{1}{2} = 0 \tag{2a}$$

$$-\frac{3}{2}\left[\left(\frac{1}{2}\cos^3\frac{\theta}{2} - \cos\frac{\theta}{2}\sin^2\frac{\theta}{2}\right) + \frac{1}{\mu}\left(\sin^3\frac{\theta}{2} - \frac{7}{2}\sin\frac{\theta}{2}\cos^3\frac{\theta}{2}\right)\right] < 0 \tag{2b}$$

where

$$\mu = \frac{K_I}{K_{II}} \tag{3}$$

If the stress intensity ratio is known then Eq. (2) can be solved for θ such that $\theta = \theta_0$, which is the predicted crack initiation angle.

3.2 S-criterion

Sih [17, 18] used the strain as a critical parameter in order to propose the minimum strain energy density (S) criterion. It states that the direction of crack initiation coincides with the direction of minimum strain energy density along a constant radius around the crack tip. The (S) criterion showed a good agreement with the experimental results obtained earlier by Erdogan and Sih [6]. In addition, this criterion is the only one that shows the dependence of the initiation angle on material property represented by Poisson's ratio *v*. In mathematical form, S-criterion can be stated as:

$$\begin{cases} \dfrac{\partial S}{\partial \theta} = 0 \\ \dfrac{\partial^2 S}{\partial^2 \theta} < 0 \end{cases} \tag{4}$$

where S is the strain energy density factor, defined as:

$$S = r_0 \frac{\mathrm{d}W}{\mathrm{d}V} \tag{5}$$

where $\mathrm{d}W/\mathrm{d}V$ is the strain energy density function per unit volume, and r_0 is a finite distance from the point of failure initiation. For slit cracks, the crack tip is assumed to be the point of failure initiation.

$$\begin{aligned} &\left[2(1+\kappa)\mu\right]\tan^4\frac{\theta}{2} + \left[2\kappa(1-2\mu^2) - 2\mu^2 + 10\right]\tan^3\frac{\theta}{2} - 24\mu\tan^2\frac{\theta}{2} \\ &\qquad + \left[2\kappa(1-\mu^2) + 6\mu^2 - 14\right]\tan\frac{\theta}{2} + 2(3-\kappa)\mu = 0 \end{aligned} \tag{6a}$$

$$\left[2(\kappa-1)\mu\right]\sin\theta - 8\mu\sin 2\theta + \left[\left((\kappa-1)\right)(1-\mu^2)\right]\cos\theta + \left[2(\mu^2-3)\right]\cos 2\theta < 0 \tag{6b}$$

where μ is defined as in Eq. (3). Similar to MTS criterion, after finding the stress intensity ratio μ, Eq. (6) can be solved for θ, $\theta = \theta_0$ which is the predicted crack initiation angle.

3.3 T-criterion

Similar to Sih, Theocaris et al. [21-23] used the strain as a critical parameter to propose the maximum dilatational strain energy (T) criterion. It states that the direction of crack initiation coincides with the direction of maximum dilatational strain energy density along the contour of constant distortional strain energy around the crack tip. Theocaris et al. [21-23] used Polycarbonate specimens for their experimental work and their experimental results showed a good agreement with the theoretical predictions. In mathematical form, T-criterion can be stated as:

$$\begin{cases} \dfrac{\partial T_v}{\partial \theta} = 0 \\ \dfrac{\partial^2 T_v}{\partial^2 \theta} = 0 \end{cases} \tag{7}$$

$$\tan^5\frac{\theta}{2} - 4\mu\tan^4\frac{\theta}{2} + (5\mu^2 - 1)\tan^3\frac{\theta}{2} + \frac{(3-5\mu^2)\mu}{2}\tan^2\frac{\theta}{2} + \frac{(\mu^4 - 2\mu^2 - 1)}{2}\tan\frac{\theta}{2} + \frac{(1+\mu^2)\mu}{2} = 0 \tag{8a}$$

$$\left[1 - 20\mu^2 - 5\mu^4\right]\cos\theta + \left[8(3 + 2\mu^2 - \mu^4)\right]\cos 2\theta - \left[3(3 - 12\mu^2 + \mu^4)\right]\cos 3\theta + \left[2(13 + 5\mu^2)\mu\right]\sin\theta + \left[32(1 + \mu^2)\mu\right]\sin 2\theta - \left[6(5 - 3\mu^2)\mu\right]\sin 3\theta < 0 \tag{8b}$$

Again the same procedure as for MTS can be applied to find the crack initiation angle.

3.4 M-criterion

Kong et al. [11] proposed the maximum stress triaxiality (M) criterion which uses the stress as a critical parameter. It states that the direction of crack initiation coincides with the direction of maximum stress triaxiality ratio along a constant radius around the crack tip. Kong et al. [11] performed experiments using steel (FeE550) specimen at low temperature (-140ºC) in order to ensure that K controls the fracture. Kong et al. [11] experimental results were in agreement with the theoretical predictions as well as the experimental results by Theocaris et al. [21-23] and T criterion. M-criterion can be stated mathematically as:

$$\begin{cases} \dfrac{\partial M}{\partial \theta} = 0 \\ \dfrac{\partial^2 M}{\partial^2 \theta} < 0 \end{cases} \tag{9}$$

$$\tan^4\frac{\theta}{2} - 3\mu\tan^3\frac{\theta}{2} - (1 - 2\mu^2)\tan^2\frac{\theta}{2} + \frac{1}{2}(1 - \mu^2)\mu\tan\frac{\theta}{2} - \frac{1}{2}(1 + \mu^2) = 0 \tag{10a}$$

$$\left[2(\mu^2 + 5)\right]\sin\frac{\theta}{2} + \left[27(\mu^2 + 1)\right]\sin\frac{3\theta}{2} + \left[5(5\mu^2 - 3)\right]\sin\frac{5\theta}{2} - \left[2(\mu^2 + 5)\right]\cos\frac{\theta}{2} - \left[9(\mu^2 + 1)\mu\right]\cos\frac{3\theta}{2} - \left[5(5\mu^2 - 7)\mu\right]\cos\frac{5\theta}{2} < 0 \tag{10b}$$

Although plane strain formulation is done here, however, plane stress formulation gives the same results. Again the same procedure as for MTS is applied to find the crack initiation angle.

3.5 Modified MTS criterion

Shafique and Marwan [19] modified the MTS criterion in order to be suitable for analyzing ductile materials. To achieve this, they introduced a variable radius for the plastic core region and used the von Mises yield criterion for determining the variable radius.

$$12\tan^6\frac{\theta}{2}-24\mu\tan^5\frac{\theta}{2}+\left[3+16\mu^2\right]\tan^4\frac{\theta}{2}-\left[\left(5+4\mu^2\right)\mu\right]\tan^3\frac{\theta}{2}+3\mu^2\tan^2\frac{\theta}{2}$$
$$-\frac{\left[(7+5\mu^2)\mu\right]}{2}\tan\frac{\theta}{2}-\frac{(9+5\mu^2)}{2}=0 \tag{11a}$$

$$\left[(177+49\mu^2)\right]\sin\frac{\theta}{2}+\left[(1269+621\mu^2)\right]\sin\frac{3\theta}{2}-\left[(255+425\mu^2)\right]\sin\frac{5\theta}{2}$$
$$-\left[(189+147\mu^2)\right]\sin\frac{7\theta}{2}-\left[(305+49\mu^2)\mu\right]\cos\frac{\theta}{2}-\left[(423+207\mu^2)\mu\right]\cos\frac{3\theta}{2} \tag{11b}$$
$$-\left[(595-85\mu^2)\mu\right]\cos\frac{5\theta}{2}-\left[(315-21\mu^2)\mu\right]\cos\frac{7\theta}{2}<0$$

3.6 R-criterion

Shafique and Marwan [20] proposed the (R) criterion which states that the direction of the crack initiation angle coincides with the direction of the minimum distance from the crack tip to the core region boundary. Mathematically, the R criterion can be stated as:

$$\begin{cases}\dfrac{\partial R_P}{\partial\theta}=0\\ \dfrac{\partial^2 R_P}{\partial^\theta\theta}<0\end{cases} \tag{12}$$

$$2\mu\tan^4\frac{\theta}{2}+(5-2\mu^2)\tan^3\frac{\theta}{2}-9\mu\tan^2\frac{\theta}{2}+(\mu^2-4)\tan\frac{\theta}{2}+\mu=0 \tag{13a}$$

$$(1-\mu^2)\cos\theta+3(1-\mu^2)\cos2\theta+2\mu\sin\theta-12\mu\sin2\theta>0 \tag{13b}$$

Again the same procedure as for MTS can be applied to find the crack initiation angle. Graeffe's root squaring method has been used to solve the equations of all the crack initiation criterions. This method has an advantage over the other methods that it does not require any prior information about the roots and is applicable to solve polynomial equations of higher degree and is also capable of giving all the roots. However, another method called Descarte's rule of sign was used to determine the maximum number of positive and negative roots. This method states that the equation $f(x)=0$ cannot have more positive roots than the changes of sign in $f(x)$ and more negative roots than the changes of sign $f(-x)$.

4 GRAEFFE'S ROOT SQUARING METHOD

This method has an advantage over the other methods that it does not require any prior information about the roots. But it is applicable to solve polynomial equations of higher degree as in this case and is also capable of giving all the roots. The polynomial equation can be written as,

$$x^n+a_1x^{n-1}+a_2x^{n-2}+.....+a_{n-1}x+a_n=0 \tag{14}$$

Separating the even and odd powers of x and squaring, we get

$$(x^n+a_2x^{n-2}+a_4x^{n-4}....)^2=(a_1x^{n-1}+a_3x^{n-3}+....)^2 \tag{15}$$

Substituting $x^2=y,$ and simplifying, the new equation becomes

$$y^n+b_1y^{n-1}+.....+b_{n-1}y+b_n=0 \tag{16}$$

where

$$\begin{cases} b_1 = -a_1^2 + 2a_2 \\ b_1 = a_2^2 - 2a_1a_3 + 2a_4 \\ b_n = (-1)^n a_n^2 \end{cases} \tag{17}$$

If $\alpha_1, \alpha_2, ...\alpha_n$ be the roots of Eq. (14) then the roots of Eq. (15) are $\alpha_1^2, \alpha_2^2, ...\alpha_n^2$. After *m* squaring, let the new transformed equation be

$$z^n + c_1 z^{n-1} + ... + c^{n-1} z + c_n = 0 \tag{18b}$$

whose roots $\gamma_1, \gamma_2 ....\gamma_n$ are such that

$$\gamma_i = \alpha_i^{2m}, i = 1, 2, ...n \tag{18a}$$

Assuming that $|\alpha_1| > |\alpha_1| > ..... > |\alpha_n|$, then, $|\gamma_1| >> |\gamma_2| >> ....|\gamma_n|.$, where $>>$ stands for 'much greater than', thus, $\frac{|\gamma_2|}{|\gamma_1|} = \frac{\gamma_2}{\gamma_1} = \frac{\gamma_n}{\gamma_{n-1}}$ are negligible compared to unity. Also γ_i being an even power of α_i is always positive. From Eq. (18a) we have,

$$\begin{aligned} &\sum \gamma_1 = -c_1 \text{ , i.e. } -c_1 = -\gamma_1 \left(1 + \frac{\gamma_2}{\gamma_1} + \frac{\gamma_3}{\gamma_1} + ...\right) \\ &\sum \gamma_1\gamma_2 = c_2 \text{ , i.e. } \gamma_1\gamma_2 = \left(1 + \frac{\gamma_3}{\gamma_1} + ...\right) \\ &\sum \gamma_1\gamma_2\gamma_3 = -c_3 \text{ , i.e., } c_3 = -\gamma_1\gamma_2\gamma_3 \left(1 + \frac{\gamma_4}{\gamma_1} + ...\right) \end{aligned} \tag{19}$$

i.e.

$$\gamma_1\gamma_2 .....\gamma_n = (-1)^n c_n, \qquad c_n = (-1)^n \gamma_1\gamma_2 .....\gamma_n$$

Hence by (19), we get $c_1 \approx -\gamma_1, c_2 \approx \gamma_1\gamma_2, c_3 \approx \gamma_1\gamma_2\gamma_3,$ i.e. $\gamma_1 \approx -c_1,\ \gamma_2 \approx -c_2 / c_1,\ \gamma_3 \approx -c_3 / c_2, ...\gamma_n \approx -c_n / c_{n-1}.$

In this way, this method can be used to calculate the roots of higher order polynomial equations. Out of the several roots only those roots which satisfy the inequality were considered.

5 FINITE ELEMENT MODELLING

Any crack tip has an associated least dimension (LD) factor. It can be defined as an approximate radius of the largest circle, centered at the crack tip; within which no geometrical or applied load quantity varies Abdalla et al. [1] surrounding the crack tip within which the singular stress field can be guaranteed to dominate the solution. This imaginary circle is related to the following important parameters. Firstly, if the crack has some radius of curvature close to the crack tip, then the singularity can dominate the solution only within a region of radius which is some small percentage of the radius of curvature of the crack. Therefore the crack radius of curvature is one of the quantities which should be considered in computing the crack tip Least Dimension (LD). In the present study, no blunting of crack is considered. Therefore, the effect of radius of curvature was neglected. Secondly, the applied loading can also affect the size of the region surrounding the crack tip in which the singular term in the stress field dominates the solution. If a point load is applied near the crack tip, it can distort the stress field locally. Therefore, the region in which the singular terms dominate the stress field should not contain any point loads. In this case, there is no such point load applied in the vicinity of crack tip instead the load is applied on top and bottom edge of the

specimen and thus satisfied the condition. Thirdly, LD must be selected small enough so that the distance to the nearest material discontinuity or geometrical discontinuity could significantly affect within the region of radius of LD. In this study, the crack tip was approached close to the boundary of the specimen when *a/w* ratio taken to 0.7 so the radius of element rows selected in such a way that it is not affected by the boundary close to the crack tip. Lastly, after finite element analysis of linear elastic problem has been performed the numerically calculated stress field near the crack tip should evidence the necessary $r^{-1/2}$ radial distribution of stress.

5.1 Modeling

5.1.1 Geometry

In the case of an inclined crack, the model was not symmetric. Thus, full model of the edge cracked plate was analyzed using ANSYS 11 environment. The problem was idealized as 2D plane stress and the geometry was modeled using 8 keypoints with keypoint 7 being the crack tip. Keypoints 6 and 8 are coincident such that each one belonging to opposite crack face as shown in Fig. 1. Edge crack specimen was modeled with same crack length but different angle of inclination. The inclination angles considered in this study are 0°, 15°, 30°, 45° and 50°.

5.1.2 Material model and element type

Araldite-hardener was modeled as a linear isotropic material with elastic modulus 1.99 GPa and Poisson's ratio 0.36 obtained experimentally. But since the problem is idealized as two dimensional, therefore PLANE183 triangular 6 noded structural element having two degrees of freedom in *x* and *y* directions have been used for FE modeling. It is a higher order element and possesses quadratic displacement behavior and is well suited to modeling irregular meshes shown in Fig. 3. This element is defined by 8 nodes or 6-nodes having two degrees of freedom at each node: translations in the nodal *x* and *y* directions. In addition to this, element behavior was chosen to plane stress (as the problem is 2D) along with thickness to 6.5 mm as a real constant.

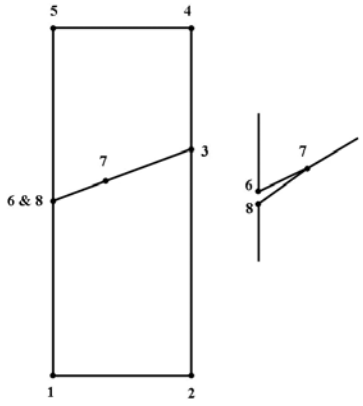

Fig. 1
Position of keypoints and lines at crack.

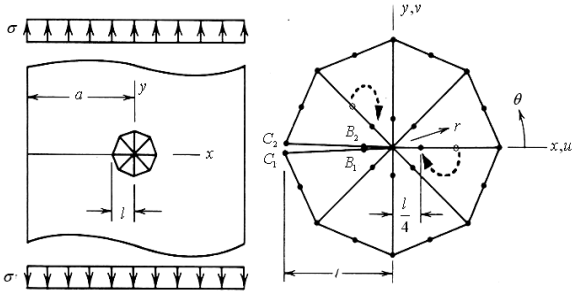

Fig. 2
Quarter node element at crack tip.

5.1.3 Finite element mesh

A typical finite element mesh for the 2-D analysis is depicted in Fig. 3 which has elements and nodes shown in Table 1 to unsymmetrical full model of the edge crack panel is modeled. To avoid problems of incompressibility, 6 noded quadratic triangular elements whose mid side nodes have been shifted to the quarter-points of the element sides (element type PLANE183 for plane stress condition with ANSYS library) are used for 2-D shown in Fig. 2. Convergence of mesh is carried out shown in Fig. 4 to get more accurate results. The radius of the concentration point is chosen to 0.8 mm and its location is at keypoint 7 depicted in Figs. 1 and 2. On the other hand, the ratio of the second row elements radius to the first row elements radius are selected to be 0.5 and the element size was considered to be 0.003. The number of elements in circumferential direction is selected to 6 which have created 12 singular elements around the crack tip. The specifications of the crack tip mesh and a close up view for crack inclination angles β=45º are shown in Fig. 3.

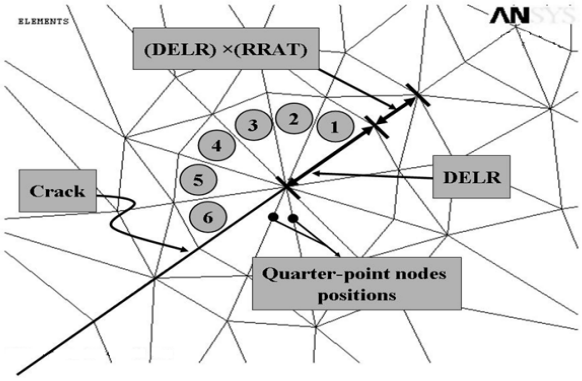

Fig. 3
Crack tip mesh.

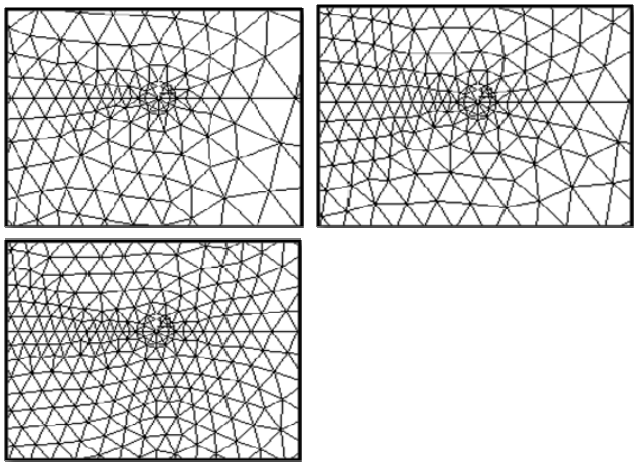

Fig. 4
Convergence of mesh at crack tip.

Table 1
FE Model specifications and numerically obtained SIF

Angle (β)	Element	Nodes	K_I (MPa)	K_{II} (MPa)	K_{II}/K_I	K_I/K_{II}
0˚	1906	2561	3.07	0.0	0	0
15˚	1943	2720	2.70	0.35	0.13	7.71
30˚	1969	2920	2.35	0.65	0.27	3.61
45˚	2081	3189	1.40	0.64	0.45	2.18
50˚	2157	3427	1.36	0.72	0.53	1.90

5.1.4 Loading and boundary conditions

Pressure boundary condition is prescribed on the top surface of the model while the bottom surface is restricted in the *y*-direction and one node, at *x*=0 and *y*=0, is restricted in *x* and *y* direction as shown in Fig. 5. Table 2 gives the different values of critical pressure applied on the specimen at different β, until the fracture of specimen occurs to obtain the critical value of mixed mode stress intensity factors.

5.1.5 Crack path modeling

Since a full model is considered, five nodes need to be selected along the two crack faces to get the value of mixed mode stress intensity factors K_I and K_{II}. The first node should be the crack tip and the second and third nodes are the first and second nodes next to the crack tip on the crack's top face. The forth and fifth nodes have to be the first and second nodes next to the crack tip but on the crack's bottom face as shown in Fig. 6.

6 ANALYTICAL VERIFICATION OF MODE I SIF

There are closed form solutions available for calculating the SIF for single edge crack panel but for pure opening mode I SIF. The general form can be represented as:

$$K_I = Y\sigma\sqrt{a} \tag{20}$$

where Y is the geometry correction factor and it is usually a function of both crack length a and panel width w. The available geometry factor is only valid for a straight single edge crack panel and is calculated as:

$$Y = 1.99 - 0.41\left(\frac{a}{w}\right) + 18.7\left(\frac{a}{w}\right)^2 - 38.48\left(\frac{a}{w}\right)^3 + 53.85\left(\frac{a}{w}\right)^4 \tag{21}$$

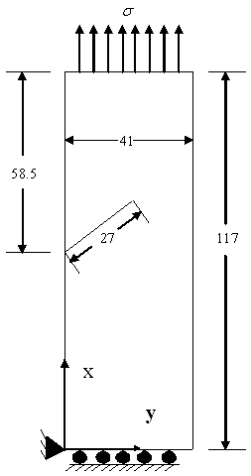

Fig. 5
Inclined crack panel with boundary condition.

Table 2
Mixed mode SIF obtained from *J*-Integral

β°	Critical Load(N)	Critical Stress (MPa)	K_I (MPa)	K_{II} (MPa)	K_{II}/K_I	K_I/K_{II}
0°	515.99	1.92	3.51	0	0	0
15°	551.57	2.06	3.10	0.26	0.10	11.92
30°	716.16	2.67	2.67	0.57	0.22	4.68
45°	782.88	2.92	1.60	0.47	0.30	3.40
50°	969.71	3.62	1.54	0.58	0.52	2.5

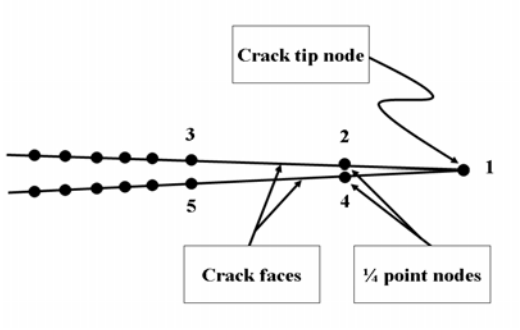

Fig. 6
Crack path definition of opening crack.

Crack length (a) considered for the mode I case is taken to 27.5 mm, and the panel width is 41 mm, yields a/w ratio to 0.67. By substituting the value of a/w ratio in Eq. (27), the value of Y yields to 7.571. Substituting the value of Y and applied stress in Eq. (26), yields the value of K_I to 2.8 MPa which is very close to the value of K_I obtained by FEA shown in Table 1. This validates the correctness of mode I SIF obtained using finite element analysis.

7 *J*-INTEGRAL BASED APPROACH

Within the framework of plane linear fracture mechanics, many different approaches to the computation of critical parameters associated with crack extension have been proposed. Among these methods, Rice's J-integral is extremely attractive since it involves only the evaluation of a path independent contour integral. The method is easily incorporated into most existing finite element stress analysis programs which have no provision for treating singular stress states. Charepanov [5] investigated that the components of two dimensional J-integral shown in Fig. 7 are defined as

$$J_K = \lim_{\varepsilon \to 0} \int_{\Gamma_\varepsilon} \left[W n_k - \sigma_{ij} \frac{\partial u_i}{\partial x_k} n_j \right] \mathrm{d}\Gamma \tag{22}$$

where W is the stress work density, σ_{ij} are stresses, u_i are displacements and n_k is the unit outward normal to the contour (Γ_ε). If an arbitrary but continuous function $s(x_1, x_2)$ is chosen such that

$$\begin{cases} s = 1 \ \text{ on } \ \Gamma_\varepsilon \\ s = 0 \ \text{ on } \ \Gamma_a \end{cases} \tag{23}$$

where Γ_ε, and Γ_a, are illustrated in Fig. 7, and introduce the notation

$$J_k^{\Gamma} = \int_{\Gamma} \left[W n_k - \sigma_{ij} \frac{\partial u_i}{\partial x_k} n_j \right] \mathrm{d}\Gamma \tag{24a}$$

$$J_k^{\Gamma,s} = \int_{\Gamma} \left[W n_k - \sigma_{ij} \frac{\partial u_i}{\partial x_k} n_j \right] s \ \mathrm{d}\Gamma \tag{24b}$$

The function s was chosen in linear form and introduced by means of shape functions N as reads

$$s = N^M s^M \tag{25}$$

where superscript M refers to the node number and

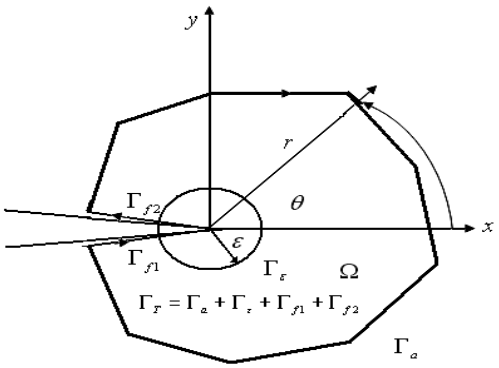

Fig. 7
Coordinate systems and *J*-integration contours.

$$s^M = \begin{cases} 1 \text{ ... at the crack tip} \\ 0.75 \text{ or } 0.5 \text{ ... at a shift} \quad \text{or} \quad \text{non-shifted midside node respectively} \\ 0 \text{ ... at the remaining element nodes} \end{cases}$$

It can be seen in Fig. 7 that,

$$J_k^{\Gamma,\varepsilon} = J_k^{\Gamma_{1,s}} - J_k^{\Gamma f_{1,s}} - J_k^{\Gamma f_{2,s}} \tag{26}$$

The use of divergence theorem given by Charepanov [5] leads to

$$J_k^{\Gamma,\varepsilon} = -\int_{\Omega}\left[W\frac{\partial s}{\partial x_k} - \sigma_{ij}\frac{\partial u_i}{\partial x_k}\frac{\partial s}{\partial x_j}\right]\mathrm{d}\Omega - \int_{\Omega}\left[\frac{\partial W}{\partial x_k} - \frac{\partial}{\partial x_j}\left(\sigma_{ij}\frac{\partial u_i}{\partial x_k}\right)\right]s\ \mathrm{d}\Omega - (J_k^{\Gamma_{f1,s}} + J_k^{\Gamma_{f2,s}}) \tag{27}$$

where Ω designates the domain enclosed by the contour Γ_t. Accepting the assumptions of elastic continuum, small deformation theory, and the absence of body forces and temperature loading which are sufficient conditions to make the second term in Eq. (27) zero. At the same time the presupposition of traction-free crack faces are accepted and noticed the properties of the quantities indicated so far under the above described conditions for k = 1 and k =2. Obviously it holds,

$$J_I^{\Gamma_{f1,s}} = J_I^{\Gamma_{f2,s}} = 0 \tag{28}$$

Thus,

$$J_I^{\Gamma,\varepsilon} = -\int_{\Omega}\left[W\frac{\partial s}{\partial x_1} - \sigma_{ij}\frac{\partial u_i}{\partial x_1}\frac{\partial s}{\partial x_j}\right]\mathrm{d}\Omega \tag{29}$$

Irrespective of the width and distance of domain Ω from the crack tip, and also according to Eq. (22)

$$J_I = -\int_{\Omega}\left[W\frac{\partial s}{\partial x_1} - \sigma_{ij}\frac{\partial u_i}{\partial x_1}\frac{\partial s}{\partial x_j}\right]\mathrm{d}\Omega \tag{30}$$

If the domain Ω is close to the crack tip, then the displacements and stresses will, with appropriate accuracy, comply with an asymptotic solution and

$$J_I^{\Gamma_{f1,s}} + J_I^{\Gamma_{f2,s}} \approx 0 \tag{31}$$

Then according to Eq. (22, 27and 31) it can be written as

$$J_{II} \approx -\int_{\Omega}\left[W\frac{\partial s}{\partial x_2} - \sigma_{ij}\frac{\partial u_i}{\partial x_2}\frac{\partial s}{\partial x_j}\right]\mathrm{d}\Omega \tag{32}$$

The validity of Eq. (32) is the more accurate, the closer the crack tip is surrounded by the domain Ω. Between the *J*-integral and the SIF components hold the relationships derived, given by Charepanov [5]

$$\begin{cases} J_I = \dfrac{1}{E^*}(K_I^2 + K_{II}^2) \\ J_{II} = -\dfrac{2}{E^*}K_I K_{II} \end{cases} \tag{33}$$

From which K_I and K_{II} may be explicitly expressed

$$\begin{cases} K_I = \dfrac{1}{2}\sqrt{E^*}(\sqrt{J_I - J_{II}} + \sqrt{J_I + J_{II}}) \\ K_{II} = \dfrac{1}{2}\sqrt{E^*}(\sqrt{J_I - J_{II}} - \sqrt{J_I + J_{II}}) \end{cases} \tag{34}$$

Here $E^* = E$ for plane stress and $E^* = E/(1-\nu^2)$ for plane strain, where *E, v* are Young's modulus and Poisson's ratio, respectively. All the crack initiation angle criterion can predict the crack initiation angle θ, if the ratio of K_I / K_{II} is known but a careful investigation of Eq. (3) and Eq. (35) can lead to an important conclusion that using *J*-integral based approach crack initiation angle can be equally determined by using Eq. (36) in terms of J as

$$\mu = \frac{K_I}{K_{II}} = \frac{(\sqrt{J_I - J_{II}} + \sqrt{J_I + J_{II}})}{(\sqrt{J_I - J_{II}} - \sqrt{J_I + J_{II}})} \tag{35}$$

Eq. (36) can be further simplified as,

$$\begin{aligned} \mu = \frac{K_I}{K_{II}} &= \frac{(\sqrt{J_I - J_{II}} + \sqrt{J_I + J_{II}})}{(\sqrt{J_I - J_{II}} - \sqrt{J_I + J_{II}})} \times \frac{(\sqrt{J_I - J_{II}} + \sqrt{J_I + J_{II}})}{(\sqrt{J_I - J_{II}} + \sqrt{J_I + J_{II}})} \\ \frac{K_I}{K_{II}} &= \frac{(\sqrt{J_I - J_{II}})^2 + (\sqrt{J_I + J_{II}})^2 + 2(\sqrt{J_I - J_{II}})(\sqrt{J_I + J_{II}})}{(\sqrt{J_I - J_{II}})^2 - (\sqrt{J_I + J_{II}})^2} \\ \frac{K_I}{K_{II}} &= \frac{-J_I - (\sqrt{J_I - J_{II}})(\sqrt{J_I + J_{II}})}{J_{II}} \end{aligned} \tag{36}$$

Finally, the equation comes out in the form

$$\mu = \frac{K_I}{K_{II}} = -\left(\frac{J_I + \sqrt{J_I^2 - J_{II}^2}}{J_{II}}\right) \tag{37}$$

Thus Eq. (37) gives that the ratio of stress intensity factor is equal to the negative function of mixed mode *J*-Integral. To evaluate the *K* components, using *J*-Integral approach, in single edge crack panel depicted in Fig. 5, conventional isoparametric triangles elements with 6 nodes are used. The function*s* were chosen in linear form and introduced by means of shape functions *N* as reads by Eq. (25).

8 RESULTS AND DISCUSSION

8.1 Effects on mode I and mode II SIF

Fig. 8 gives the comparison of mode I and mode II SIF, computed numerically as well as *J*-Integral based approach with respect to crack inclination angle. It was observed that results obtained from both approach are very close to each other. In other words, both methods can be employed to determine crack initiation angle. Significant fall of curves was noticed between $\beta = 30°$ to $\beta = 48°$ after that K_I was found to increase. Table 2 shows that as β increases, higher stresses were required to fracture the specimens. Fig. 9 gives the clear picture of yielding at the crack tip. It was observed that increasing crack inclination angle implies to decreasing the equivalent von Mises stresses for all *a/w* ratio from 0.1 to 0.7, which indicated that the yielding, at crack tip, decreases as β increases or in other words the stiffness of the material increases followed by rising in stress triaxiality thus trigger the chance of brittle fracture. This phenomenon can also be observed in Fig. 10 (*a* to *e*). It indicated that shrinkage of yield envelope was observed near the crack tip thus decreasing the amount of plastic zone at the crack tip and gives rise to brittle fracture.

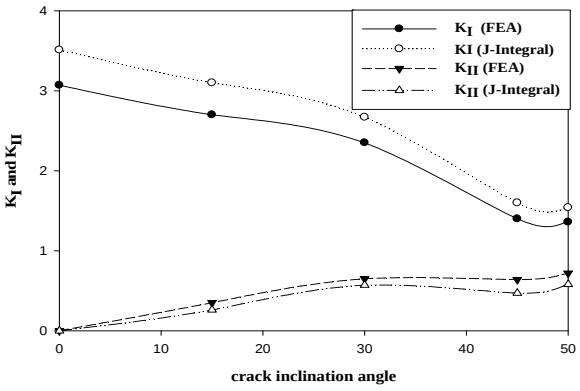

Fig. 8
Mode I and mode II SIF vs. β.

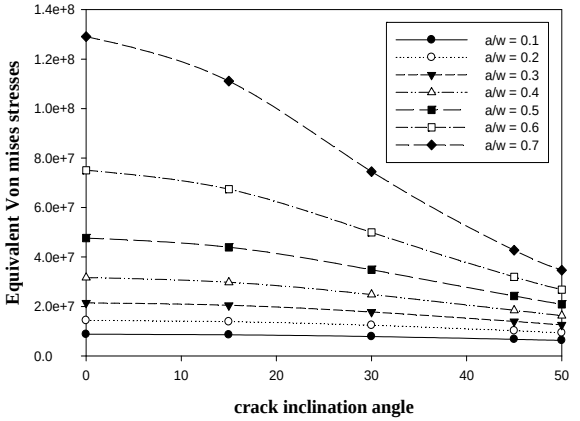

Fig. 9
Von Mises stress at the crack tip.

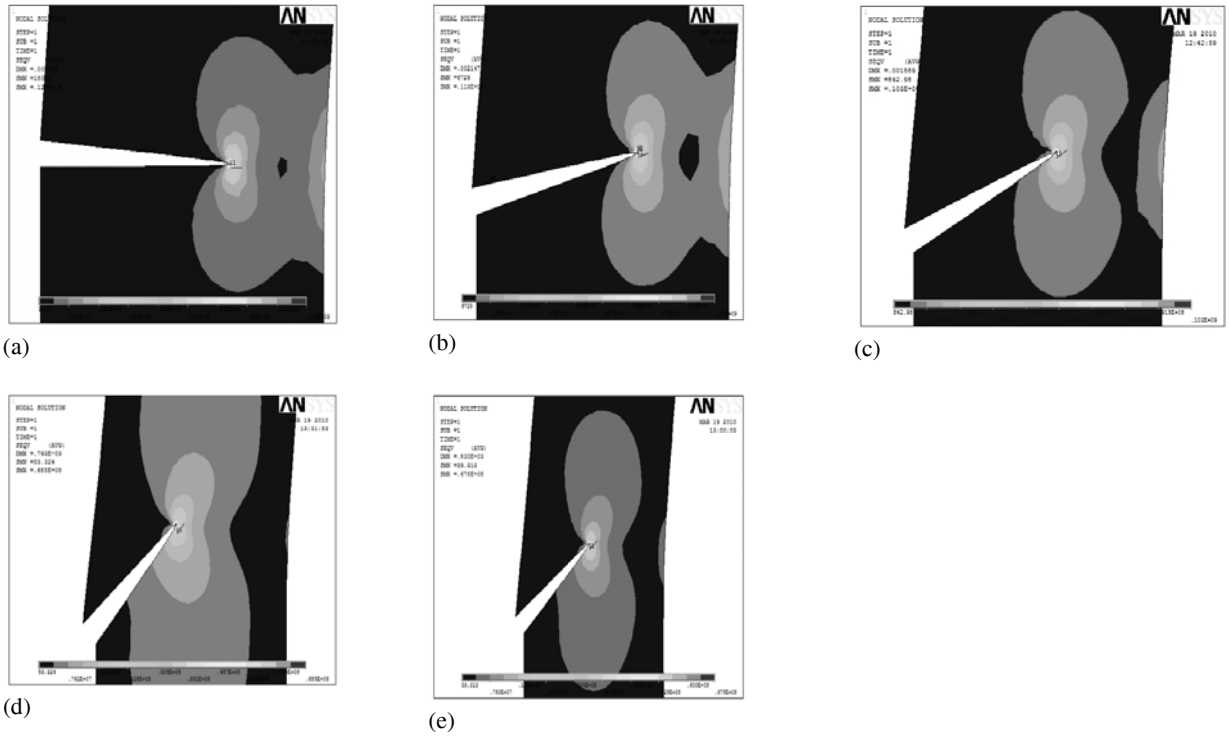

Fig. 10
Von Mises stress distribution at crack tip at: (a) 0˚ (b) 15˚ (c) 30˚ (d) 45˚ and (e) 50˚.

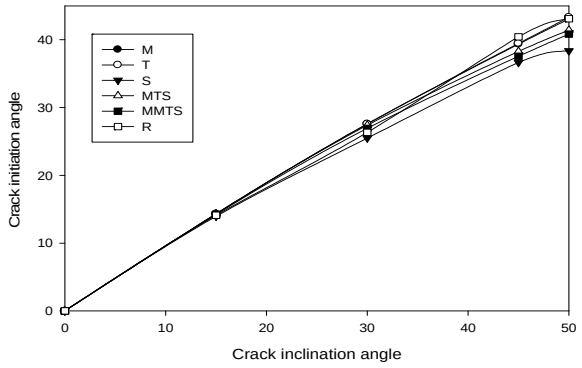

Fig. 11
Crack initiation criteria at different β.

8.2 Prediction of crack initiation angle

Stress intensity factors K_I and K_{II} were computed numerically as well as *J*-Integral based approach. These are incorporated into six crack initiation angle criteria to predict the crack propagation angle. Fig. 11 depicts that all criterion predict approximately the same crack initiation angle for the cases of small crack inclination angles (β = 0º and β = 15º). Similarly Table 3 and Fig. 12 depict the comparative study of crack initiation angles carried out by using both *K* and *J* based approaches in which a difference of about 3° was noticed if *J*-Integral based approach is followed. It is investigated that both M and T criteria were found to yield the same initiation angle for all crack angles. To support their criterion, Kong et al. [11] performed experiments on FeE550 steel center crack specimens at low temperature (-140ºC) in order to ensure that *K* controls the fracture. The authors conclude that the theoretical results of the M criterion compared very well with the experiment results of Theocaris et al. [21-23] and the T criterion. Kong et al. [11] experimental results were also in a good agreement with T criterion and the experimental results of Theocaris et al. [21-23], especially for small inclination angles.

Table 3
Comparison of *K* and *J*-Integral based Crack initiation angle obtained from different criteria

B	Crack initiation angle (-θ)											
	Numerical											
	M	T	S	MTS	MMTS	R	M	T	S	MTS	MMTS	R
0°	0	0	0	0	0	0	0	0	0	0	0	0
15°	14.318	14.318	13.958	14.315	14.228	13.85	11.91	11.78	11.91	11.91	11.88	11.84
30°	27.583	27.587	25.487	27.395	26.935	27.66	25.28	24.14	25.35	25.34	25.0	24.63
45°	39.351	39.459	36.645	38.276	37.561	33.76	32.22	30.67	32.35	32.35	32.84	30.35
50°	43.057	43.322	38.373	41.420	40.845	36.84	36.03	33.10	36.61	36.64	35.35	34.05

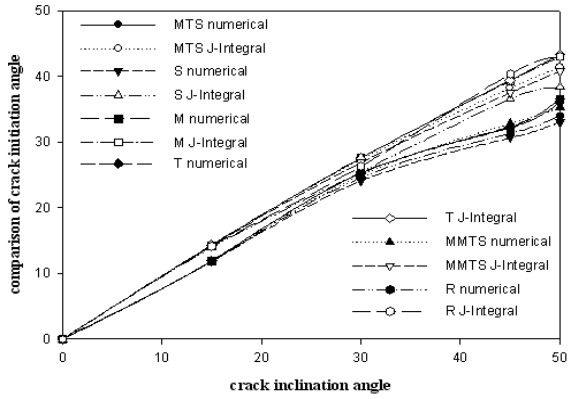

Fig. 12
Comparison of crack initiation angle obtained from K and J-Integral based approach.

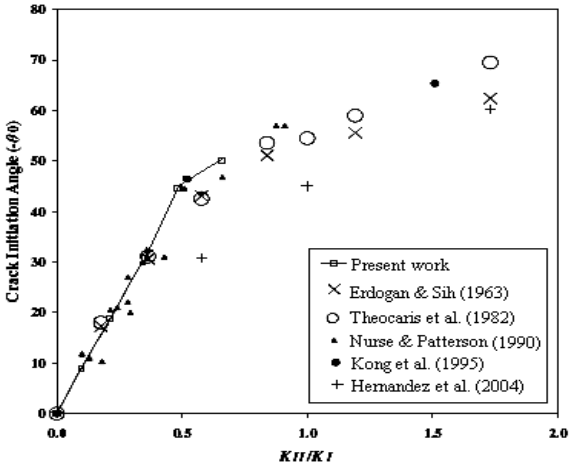

Fig. 13
Comparison of crack initiation angle of this study and available results.

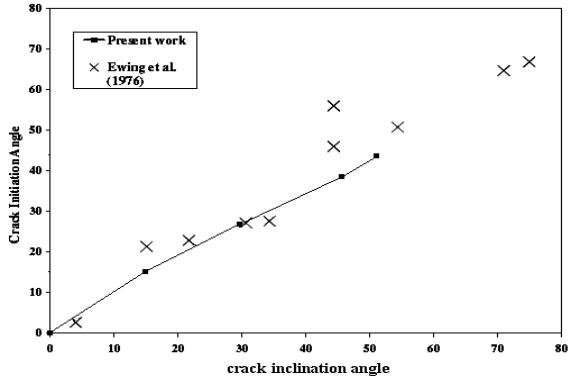

Fig. 14
Comparison between crack initiation angle of this study and Zwing et al. (1976).

Furthermore, the M and T criteria were found to predict the maximum initiation angle while the S criterion predicted the minimum angle. The same behavior of the S criterion is observed in the literature shown in Fig. 13. Zwing et al. [26] conducted experiments on PMMA edge crack specimens. Similar behavior is observed by Theocaris et al. [21-23] except that their experimental results showed an agreement with MTS and S criteria for inclination angles less than 50º shown in Fig. 14. However, their experimental measurements of the crack initiation angles showed a good agreement with T criterion for higher inclination angles.

9 CONCLUSIONS

The pure opening mode and mixed mode stress intensity factor were estimated numerically using FE code as well as *J*-Integral based approach. For pure mode, the FE model compared very well with analytical solution. After estimating K_I and K_{II}, the SIF values are incorporated into six crack initiation criteria for crack initiation prediction. All criteria give the same initiation angle between β equals to (0º to 15º). However, as the crack angle of inclination increases with an increment of 15 ° the difference in crack initiation angle prediction increases reaching more than 13º. For all inclination angles, the S criterion was found to predict the minimum initiation angle and can also gives the relationship of ductile and brittle behavior of material while both M and T criteria were found to predict the maximum initiation angle. The crack initiation angle obtained using stress intensity factor and *J*-integral based approach are close to each other and also found to be in good agreement with the available experimental results in literature. It was also observed that as crack inclination angle increases material is found to behave as brittle fracture.

REFERENCES

[1] Abdalla J.E., Gerstle W.H., 1988, A finite element for arbitrarily precise determination of stress intensity factors, *Bureau Of Engineering Report* **CE-84**(88), College of Engineering, University of New Mexico, Albuquerque.

[2] Ayhan A.O., 2004, Mixed mode stress intensity factors for deflected and inclined surface cracks in finite-thickness plates, *Engineering Fracture Mech*anics **71**: 1059-1079.

[3] Barsoum R.S., 1976, On the use of isoparametric finite elements in linear fracture mechanics, *International Journal for Numerical Methods in Engineering* **10**: 25-37.

[4] Barsoum R.S., 1977, Triangular quarter-point elements as elastic and perfectly plastic crack tip elements, *International Journal for Numerical Methods in Engineering* **11**: 85-98.

[5] Cherepanov G.P., 1974, *Mechanics of Brittle Fracture*, Nauka, Moscow, (in Russian).

[6] Erdogan F., Shi G.C., 1963, On the crack extension in plates under plane loading and transverse shear, *Journal of Basic Engineering* **85**: 519-527.

[7] Griffith A.A., 1921, The phenomena of rupture and flow in solids, *Philosophical Transactions of the Royal Society of London*, Series A221, pp. 199.

[8] Henshell R.D., Shaw K.G., 1975, Crack tip finite element are unnecessary, *International Journal for Numerical Methods in Engineering* **9**: 495-507.

[9] Josh J., Ptaik S, 1989, On stress intensity factor computation by finite element method under mixed mode loading conditions, *Engineering Fracture Mech*anics **34**(1): 169-177.

[10] Knesl Z., 1988, Stress intensity factor computing under mixed mode loading conditions by the use of energy release rate (in Czech). *Strojirenstvi* **37**: 163-166

[11] Kong X.M., Schluter N., Dahl W., 1995, Effect of triaxial stress on mixed mode-facture, *Engineering Fracture Mech*anics **52**(2) :379-388.

[12] Owen D.R.J., Fawkes A. J., 1983, *Engineering Fracture Mechanics-Numerical Methods and Applications*, Pineridge Press, Swansea, UK.

[13] Pu S.L., Hussain M.A., Lorenson W.E., 1978, The collapse cubic isoparamteric elements as singular elements for crack problems, *International Journal for Numerical Methods in Engineering* **12**: 1727-1742.

[14] Peter M., Haefele, Lee James D., 1995, Combination of finite element analyses and analytical crack tip solution for mixed mode fracture, *Engineering Fracture Mech*anics **50**(5/6): 849-868.

[15] Petit C., Vergne A., Zhang X., 1996, A comparative numerical review of cracked materials, *Engineering Fracture Mech*anics **54** (3): 423-439.

[16] Rousseau C.E., Tippur H.V., 2000, compositionally graded materials with cracks normal to the elastic gradient, *Acta Materialia* **48**: 4021- 4033.

[17] Sih G.C., 1974, Strain energy density factor applied to mixed mode crack problems, *International Journal of Fracture* **10** (3): 305-321.

[18] Sih G.C., 1973, Some basic problems in fracture mechanics and new concepts, *Engineering Fracture Mech*anics **5**: 365-377.

[19] Shafique M.A., Marwan K., 2000, Analyses of mixed mode crack initiation angles under various loading conditions, *Engineering Fracture Mech*anics **67**: 397-419.
[20] Shafique M.A., Marwan K., 2004, A new criterion for mixed mode fracture initiation based on crack tip plastic core region, *International Journal of Plasticity* **20**: 55-84.
[21] Theocaris P.S., Andrianopoulos N.P. 1982, The T-criterion applied to ductile fracture, *International Journal of Fracture* **20**: 125-130.
[22] Theocaris P.S., Andrianopoulos N.P., 1982, The Mises elastic-plastic boundary as the core region in fracture criteria, *Engineering Fracture Mechanics* **16**: 425-432.
[23] Theocaris P.S., Kardomateas G.A., Andrianopoulos N.P., 1982, Experimental study of the T-criterion in ductile fracture, *Engineering Fracture Mechanics* **17**: 439-447.
[24] Tilbrook M.T., Reimanis I.E., Rozenburg K., Hoffman M., 2005, Effect of plastic yielding on crack propagation near ductile/brittle interfaces, *Acta Materialia* **53**: 3935-3949.
[25] Ukadgaonker V.G., Awasare P.J., 1995, A new criterion for fracture initiation, *Engineering Fracture Mech*anics **51** (2): 265-274.
[26] Zwing P.D., Swedlow J.L., Williams J.G., 1976, Further results on the angled crack problem, *International Journal of Fracture* **12**(1):85-93.